# Comments on the Scaling Behavior of Flexible Polyelectrolytes within the Debye−Hückel Approximation†

**Magnus Ullner***

*Physical Chemistry 1, Center for Chemistry and Chemical Engineering, Lund University, P.O. Box 124, S-221 00 Lund, Sweden*

*Received: November 3, 2002; In Final Form: April 22, 2003*

Over the years, there has been much debate regarding the conformational behavior of flexible polyelectrolytes with electrostatic interactions described by the Debye−Hückel approximation. In particular, the electrostatic persistence length has been reported to depend both quadratically and linearly on the screening length as well as having no consistent power-law dependence at all. On the basis of simulation results together with a careful analysis of analytical approaches, including Odijk−Skolnick−Fixman (OSF) theory, variational calculations, and renormalization group results, it is possible to present a consistent picture, which contains a better understanding of the true behavior as well as an explanation for the diverse results. The projection length of long chains can be described by power laws in three regimes, and an expression by Odijk is qualitatively correct in two of these regimes. Scaling arguments based on OSF theory and excluded volume considerations give good agreement with the third power law, but the underlying assumptions are not entirely correct. More than one parameter is required to describe the internal chain behavior, which is characterized by short-range flexibility and long-range stiffness. Still, most analytical approaches end up in one of two one-parameter approximations, either an OSF-like perturbation expansion around a rigid-rod state or a Flory-type variational calculation based on an unperturbed chain. The latter describes at best the short-range behavior. A field-theoretic renormalization group treatment, which has suggested that there should be no power law behavior, is not valid in three dimensions. Previous support from simulation results were obtained through an unfortunate mistake.

## 1. Introduction

The conformational properties of flexible polyelectrolytes in the presence of salt has been discussed for over half a century without reaching a consensus. Most analytical theories and simulation studies treat the salt implicitly within the Debye−Hückel (DH) approximation;[1] i.e., the electrostatic interactions are described by the screened Coulomb potential

$$u_{sc}(r) = \alpha^2 k_B T l_B \frac{e^{-\kappa r}}{r} \tag{1}$$

where $\alpha$ is the degree of ionization, $k_B$ is Boltzmann's constant, $T$ is the temperature, and $l_B = e^2/(4\pi\epsilon_r\epsilon_0 k_B T)$ is the Bjerrum length, with $e$ being the elementary charge, $\epsilon_r$ the dielectric constant of the solution, and $\epsilon_0$ the permittivity of vacuum. When the polyelectrolyte is infinitely diluted and only monovalent ions are present, the Debye screening parameter is given by

$$\kappa^2 = 8\pi l_B N_A c_s \tag{2}$$

where $c_s$ is the concentration of added 1:1 salt and $N_A$ is Avogadro's number. $\kappa^{-1}$ is known as the screening length and represents the range of the (screened) electrostatic interactions.

The earliest models combined the DH approximation with the assumption that the polyion could be described as a freely jointed chain,[2−4] a tradition that has been continued by, for example, Muthukumar.[5,6] A seed of controversy was planted when Odijk[7] and Skolnick and Fixman[8] (OSF) joined the DH approximation with the wormlike-chain model.[9] This led to a simple power law. Much focus was shifted toward persistence length and a search for power laws ensued. However, the large number of investigations that followed, theoretical as well as experimental, reported a variety of results.[10] There have been two major camps as well as additional voices arguing that both camps are wrong.

Still, a consistent picture is emerging out of the diversity and it is the purpose of this paper to present this picture as well as to explain the cause of the different results.

## 2. Road Map

Due to the nature of the preceding discussions in the literature, there are several issues that need to be addressed to form a collected view. As a result, this paper may look somewhat kaleidoscopic. A detailed overview of the rest of the paper is therefore given, to show the structure and help the navigation.

3. Background

3.1. The results of Odijk−Skolnick−Fixman (OSF) theory are presented.

3.2. Different types of persistence length are defined. The snakelike-chain model is presented and related to other two-parameter models.

3.3. The general controversy regarding the conformational behavior in terms of persistence length is outlined. The two main results are referred to as OSFKK and the linear prediction.

3.4. Scaling is discussed in terms of end-to-end distance.

† Part of the special issue "International Symposium on Polyelectrolytes".

* E-mail: magnus.ullner@fkem1.lu.se.

10.1021/jp027381i CCC: $25.00 
Published on Web 06/18/2003

3.4.1. It is shown how to derive power laws that span three regimes of chain behavior given either the OSFKK picture or the linear prediction.

3.4.2. Generalized expressions are given for the simple Flory-type variational approach and for an analogous treatment related to renormalization group theory. These expressions define two general classes of results.

3.4.3. Predictions of the swelling exponents due to excluded volume interactions are discussed.

4. Methods

4.1. Descriptions are given for the simulation models and methods used to obtain the results shown in sections 5 and 7.1.

4.2. Details about the calculation of projection length from the simulations are presented.

5. Simulation Results

5.1. Empirical power laws for projection length obtained in three regimes are discussed.

5.2. Theoretical predictions are analyzed in light of the simulation results, especially the idea that flexible chains could be described by a combination of OSF theory and excluded volume considerations. It is shown that this idea is not entirely valid, although OSF theory can be applied to stiff chains in two of the regimes. The usual variational result, the linear prediction, is not valid either.

5.3. Concluding remarks for section 5 are provided.

6. Variational and Perturbational Results

6.1. Indications that the two main results stem from differences in the variational methods of Gibbs-Bogoliubov and Edwards-Singh are discarded.

6.2. It is shown that most analytical approaches rely on a single parameter and end up in one of two simple cases, an OSF-like perturbational calculation (rigid rod) or a Flory-type variational approach (completely flexible chain), which produce the two main results.

6.3. A detailed example is given of how a general approach can collapse to a simple standard case through a single approximation, while ad hoc choices determine the final result.

6.4. Comments are made on numerical results of a general Gaussian variational ansatz.

6.5. Conclusions and additional comments regarding analytical approaches are provided.

7. Field-Theoretic Renormalization Group Analysis

7.1. It is shown that a field-theoretic normalization group analysis is not applicable to three-dimensional systems. Exponents for the chain length dependence of the unscreened case are also discussed.

7.2. It is shown that, on a scaling level, the theory gives the same results as a simple Flory analysis, if (more realistic) Flory-type exponents are used instead of the renormalization group ones.

8. Conclusions

The various pieces are put together in a general summary.

## 3. Background

**3.1. Odijk−Skolnick−Fixman Theory.** Odijk[7] and Skolnick and Fixman[8] considered a stiff chain and, to first order, Odijk expressed the electrostatic contribution to the bending coefficient as

$$l_{bc,e} = \frac{(\alpha N)^2 l_B}{12}[3y^{-2} - 8y^{-3} + e^{-y}(y^{-1} + 5y^{-2} + 8y^{-3})] \quad (3)$$

with $y \equiv \kappa L$. $N$ is the number of monomers or charged sites, and $L$ is the contour length. In this approach, different contributions are additive; i.e., the total bending coefficient, $l_{bc}$, is the sum of the intrinsic, nonelectrostatic bending coefficient, $l_{bc,0}$, and the first-order electrostatic contribution,

$$l_{bc} = l_{bc,0} + l_{bc,e} \quad (4)$$

For large $y$, eq 3 reduces to[7,8]

$$l_{bc,e} = \frac{\alpha^2 l_B}{4\kappa^2 b^2} \quad (5)$$

which is the most quoted result of OSF theory and where $b$ is the contour distance between neighboring charged sites. In the salt-free case ($\kappa \rightarrow 0$), we have

$$l_{bc,e} = \frac{(\alpha N)^2 l_B}{72} \quad (6)$$

**3.2. Definitions of Persistence Length.** The bending coefficient is the parameter that governs the total bending energy of a continuous chain,

$$E_{bend} = \frac{k_B T l_{bc}}{2}\int_0^L \left(\frac{d\mathbf{u}(s)}{ds}\right)^2 ds \quad (7)$$

where $\mathbf{u}(s)$ is a unit vector in the direction of the chain at a position $s$ along the contour. With this as the only potential energy, averaging over the conformations leads to the orientational correlation function of a wormlike chain[11]

$$C(s) = e^{-s/l_{oc}} \quad (8)$$

with the orientational correlation length $l_{oc} = l_{bc}$.

Until recently,[12] $l_{bc}$ and $l_{oc}$, as defined by the two equations above, were only known under the common name of persistence length. Another property, which has also been called persistence length, is the projection length, $l_p$. It is defined as the projection of the end-to-end vector on the direction of the first bond and corresponds to an integration over the orientational correlation function. A fourth definition is the crossover distance $l_{cd}$. It represents the end-to-end distance of a subchain where an extrapolated short-range, rodlike behavior meets an extrapolated long-range flexibility. The latter can be the behavior of a freely jointed chain (Gaussian) or a self-avoiding walk (swollen). For a wormlike chain, the different definitions of persistence length are equivalent, but a polyion is not truly wormlike,[12−14] because electrostatic interactions are long-ranged and act through space rather than via the chain itself. As a result, the different definitions represent different properties, which is why the classification of different types of persistence length was introduced.[12]

Although a polyion is not wormlike, a reasonable description of the orientational correlation function can be obtained by a slight modification in the form of a two-parameter model,[12,14]

$$C(s) = C_0 e^{-s/l_{oc}} \quad (9)$$

$l_{oc}$ still represents a long-range exponential decay, while $C_0 < 1$ accounts for a reduction of the total correlation, due to a faster decay at short range. This model will be referred to as a snakelike chain. (Unlike a worm, a snake can have a detailed pattern on its back that differs from the general outline and, with the orientational correlation function in mind, the head (short-range) is different from the tail (long-range). Furthermore, a snake is scaled.)

The same idea of a division between short-range flexibility and long-range stiffness is also contained in the electrostatic blob model.[15,16] Despite the connection, there are differences between the two models.[10] For one thing, the snakelike chain represents an empirical result based on simulations and the parameter values are obtained by fitting, while the blob model contains predictions, which are of a qualitative nature.

There is also a close relation between eq 9 and the wormlike tension-field model of Barrat and Joanny.[17] In fact, they are mathematically congruent;[10,12] i.e., the two parameters of the tension-field model are directly related to $C_0$ and $l_{oc}$, respectively.

For very long chains, compared to the range of correlations, the snakelike chain gives $l_p = C_0 l_{oc}$ and the projection length is also directly related to the mean-square end-to-end distance, $\langle R^2 \rangle = 2Ll_p$ ($\langle ... \rangle$ denotes an ensemble average). Thus, the projection length is related to the Kuhn length, $l_K$, defined by $\langle R^2 \rangle = Ll_K$; i.e., $l_K = 2l_p$ for long chains.

The point is that it is important to keep track of which definition of persistence length is actually being discussed. Having said that, it is not always practical or even entirely relevant to be that specific in a general discussion. I will therefore violate my own recommendation and use the common term persistence length, denoted $l_p$, unless there is a specific point to discuss differences between definitions. To use $l_p$ both as a general symbol and specifically for projection length is not as bad as it might seem, because projection length is actually the most interesting of the definitions due to its connection to $\langle R^2 \rangle$ as well as by virtue of its properties. It is common to both simulations and experiments. A discussion about the relation to experiments can be found in ref 12, and ref 10 contains a survey of which definition was used where in theory and simulation.

**3.3. Scaling Behavior—Persistence Length.** To return to OSF theory, a major result is the appearance of a simple power law, eq 5. This is appealing in itself and facilitates comparison with experiments, among other things. It is also significant that it was presented at a point in time when more qualitative, but general, descriptions emerged, such as the electrostatic blob[15] and the concepts of scaling[18] (for an overview see ref 19). Thus, the OSF result has been associated with such descriptions in different ways. For example, the existence of a power law has often been rephrased as a statement that the persistence length "scales", hence the title of this paper. I will use the word "scaling" in the sense that a property (scaled to become dimensionless) can be expressed as a universal function of the dimensionless parameters that define the system and that this function is a power law at least in some regime (parameter range).

Khokhlov and Khachaturian[16] (KK) combined the OSF result with the blob picture, which allowed for a locally flexible chain and, thus, relaxed the requirement that the chain should be stiff at all length scales shorter than the total persistence length. As a consequence, a general result, where $l_p \sim \kappa^{-2}$ is sometimes referred to as OSFKK behavior.

Whether the OSFKK result also applies to flexible chains (as implied by the KK treatment) has been a matter of much debate. The reason is that attempts to answer the question generally lead to one of three results: OSFKK, $l_p \sim \kappa^{-1}$, or no consistent power law. There are variational calculations and other analytical theories supporting both OSFKK[20−24] and the linear prediction $l_p \sim \kappa^{-1}$.[17,21,25,26] The latter has also been a common conclusion of simulations[12,14,27−29] as well as experiments[30−34] analyzing the projection length. There was also an argument that simulations displayed no power law,[13,35] but this was shown to be due to the use of a different definition, namely the orientational correlation length.[10,14] However, when the chains are stiffened by a bond angle potential, the simulation results approach OSFKK behavior,[13,14] and recent simulations of flexible but longer chains also support the OSFKK picture.[36,37] In contrast, a field-theoretic renormalization group treatment[38,39] has advocated the lack of a power law in the regime where other theories find one.

**3.4. Scaling Behavior—End-to-End Distance.** There is also the older tradition of applying the model of a freely jointed chain and expressing the conformational behavior in terms of the end-to-end distance. In fact, the concept of scaling of polymers is often associated with finding the exponent $\nu$ of

$$\langle R^2 \rangle \sim N^{2\nu} \tag{10}$$

*3.4.1. Power Laws Related to OSFKK and the Linear Prediction.* In the end-to-end representation, OSFKK and the linear prediction can be used to give two sets of scaling laws. These sets are easily derived via a Flory-type approach and illustrate another point, namely that the screening length introduces different regimes, since it can be both large and small compared to the chain size.

The approach usually attributed to Flory[15,40] can be seen as a simplified form of Flory theory,[41,42] but was actually first used by Kuhn, Künzle, and Katchalsky.[43,44] It amounts to minimizing a free energy consisting of an energetic term and the entropy of a freely jointed (Gaussian) chain, both expressed in terms of the end-to-end distance $R$. When the screening length is much larger than the chain size, i.e., $\kappa R \ll 1$, the unscreened case may be used. In this case, the interaction term is a pure Coulomb term and the free energy is[15,43,44]

$$F \sim \frac{\alpha^2 l_B N^2}{R} + \frac{R^2}{Nb^2} \tag{11}$$

ignoring numerical constants. Minimization gives

$$R \sim \alpha^{2/3} l_B^{1/3} b^{2/3} N \tag{12}$$

which describes a rod, since the end-to-end distance grows linearly with $N$.

Here we have kept the actual bond length $b$ and the true number of segments $N$. When the screening length is comparable to the chain size or smaller, the chain may have long-range flexibility, while retaining some rodlike character locally. The latter will be represented as an effective Kuhn length $l_K$ and there are $N_K$ such Kuhn segments. These effective parameters are related to the model parameters in such a way that the contour length $L = Nb = N_K l_K$ is constant and the mean-square end-to-end distance is

$$R^2 = N_K l_K^{\,2} = Ll_K \tag{13}$$

when the interactions are confined to a certain number of segments along the contour so that the effective behavior is that of a freely jointed (Gaussian) chain with $R^2 \sim N_K$.

If the screening length is small, $\kappa R \gg 1$, the chain may be flexible enough to form loops that allow distant parts to interact occasionally. These so-called excluded volume interactions are treated by assigning an effective volume, $V_e$, to a segment, where

$V_e$ may be calculated from the pair potential. The Flory approach for excluded volume interactions gives

$$F \sim \frac{V_e {N_K}^2}{R^3} + \frac{R^2}{N_K {l_K}^2} \tag{14}$$

and

$$R \sim {V_e}^{1/5} {l_K}^{2/5} {N_K}^{3/5} = \left(\frac{V_e}{l_K}\right)^{1/5} L^{3/5} \tag{15}$$

which, in terms of $\langle R^2 \rangle \sim N^{2\nu}$, produces the classical Flory exponent $\nu = 3/5$ for a self-avoiding walk.

Odijk and Houwaart[45] made the assumption that $l_K$ can be equated with the total persistence length of OSF theory and that $V_e \sim \kappa^{-1} {l_K}^2$ in analogy with the second virial coefficient $A_2 \sim dl^2$ of rods,[46] with $d = \kappa^{-1}$ as the diameter and $l = l_K$ as the rod length. They used a more advanced excluded volume treatment, but in the asymptotic limit the result is the same as in the Flory analysis. With the total persistence length dominated by the result of eq 5, i.e., $l_K \sim \kappa^{-2}$ and $V_e \sim \kappa^{-5}$, the scaling behavior of eqs 12, 13, and 15 can be summarized as[16,19,36,37]

$$R^2 \sim N^2 \tag{16}$$

in the unscreened regime,

$$R^2 \sim \frac{N}{\kappa^2} \tag{17}$$

in the moderately screened regime without excluded volume interactions, and

$$R^2 \sim \frac{N^{6/5}}{\kappa^{6/5}} \tag{18}$$

in the excluded volume regime. The behavior with respect to the coupling parameter $\xi_p = \alpha^2 l_B / b$ is not included, because it depends on additional approximations, in particular, if the blob picture is used, as in the treatment by Khokhlov and Khachaturian.[16]

If the linear prediction, i.e., $l_K \sim \kappa^{-1}$ and $V_e \sim \kappa^{-3}$, is used instead, the result becomes[19,36,37]

$$R^2 \sim N^2 \tag{19}$$

$$R^2 \sim \frac{N}{\kappa} \tag{20}$$

and

$$R^2 \sim \frac{N^{6/5}}{\kappa^{4/5}} \tag{21}$$

respectively.

The latter power law for the excluded volume regime can also be obtained for the true chain, i.e., with $l_K = b$ and $N_K = N$, if the monomers are regarded as having a spherical volume $V_e \sim \alpha^2 l_B / \kappa^2$, which follows from an integration over the screened Coulomb potential.[47] In the present derivation, we had a rod of length $l_K \sim \kappa^{-1}$ and diameter $d \sim \kappa^{-1}$, which is also a form of spherical symmetry.

A crossover analysis[36,37] shows that the intermediate regime, eq 20, crosses over to the excluded volume behavior as soon as it appears and is therefore not observed in the end-to-end scaling of the linear prediction. The crossover distance is still $l_{cd} \sim \kappa^{-1}$; and if excluded volume effects are not included, eq 20 survives and represents the screened behavior.

While the second set of power laws, eqs 19−21, can be obtained in many different ways, eqs 17 and 18 rely on the OSFKK prediction to supply $l_K \sim \kappa^{-2}$.

Everaers et al.[36] have made a very thorough comparison between these two sets of power laws by mapping the results in a blob-renormalized parameter space. The second set, which is coupled to the linear prediction, could more or less be ruled out, while the first set, based on OSFKK, compared favorably to the simulation results. The same conclusion was also reached by Nguyen and Shklovskii[37] by analyzing one aspect of the same power laws.

*3.4.2. Generalized Expressions for Flory-Level Variational Results and Renormalization Group Results.* The Flory approach and result can be expressed in a more general way. If we have a pair potential

$$u(r) \sim \frac{\Lambda}{r^\lambda} \tag{22}$$

where $\Lambda$ is some coupling parameter, the free energy becomes

$$F \sim \frac{\Lambda N^2}{R^\lambda} + \frac{R^2}{Nb^2} \tag{23}$$

and minimization gives

$$R \sim \Lambda^{1/(\lambda+2)} b^{2/(\lambda+2)} N^{3/(\lambda+2)} \tag{24}$$

Thus, $\nu = 3/(\lambda + 2)$. In particular, since a generalization of the Coulomb potential to the spatial dimension $d$ corresponds to $\lambda = d - 2$,[18,48] the unscreened case gives $\nu = 3/d$. If the excluded volume is treated as $\lambda = d$, we have $\nu = 3/(d + 2)$.

An alternative approach to obtaining the Flory result is to insert the ansatz

$$R \sim BN^\nu \tag{25}$$

into the free energy, matching the powers of $N$ and balancing the coefficients, which is a direct consequence of the form of the free energy and the minimization procedure. The insertion gives

$$F \sim \frac{\Lambda N^2}{B^\lambda N^{\nu\lambda}} + \frac{B^2 N^{2\nu}}{Nb^2} = \frac{\Lambda N^{2-\nu\lambda}}{B^\lambda} + \frac{B^2 N^{2\nu-1}}{b^2} \tag{26}$$

Matching orders produces

$$2 - \nu\lambda = 2\nu - 1 \Leftrightarrow \nu = 3/(\lambda + 2) \tag{27}$$

and balancing coefficients leads to

$$\frac{\Lambda}{B^\lambda} = \frac{B^2}{b^2} \Leftrightarrow B = \Lambda^{1/(\lambda+2)} b^{2/(\lambda+2)} \tag{28}$$

(a minus sign is introduced, because it is really the derivatives that should be balanced and $dR^{-\lambda}/dR = -\lambda R^{-\lambda+1}$).

Combining eq 25 with eqs 27 and 28 reproduces eq 24.

One point of doing it this way is that it relates to an analysis by des Cloizeaux.[49,50] He argued that there is no reason to assume that the powers of $N$ should be matched, which is a consequence of Flory theory, since the theory neglects free energy terms that are linear in $N$ and the terms that are included in eq 23 are small in comparison. Another point is to show that

there is a one-to-one mapping of the Flory approach and an analysis performed by Bratko and Dawson[51] in Fourier space (see section 6.2).

Bratko and Dawson actually used a modified version of the method used by des Cloizeaux[49,50] and a similar mapping can be performed with respect to the result of the latter. Here, the interaction term, i.e., the first term of eq 23, better seen as a dimensionless coupling parameter, is required to be equal to 1. The first step, inserting eq 25, gives the first term of eq 26 and we have

$$\frac{\Lambda N^{2-\nu\lambda}}{B^{\lambda}} = 1 \tag{29}$$

Matching powers ($1 = N^0$),

$$2 - \nu\lambda = 0 \Leftrightarrow \nu = 2/\lambda \tag{30}$$

and balancing coefficients,

$$\frac{\Lambda}{B^{\lambda}} = 1 \Leftrightarrow B = \Lambda^{1/\lambda} \tag{31}$$

leads to

$$R \sim \Lambda^{1/\lambda} N^{2/\lambda} \tag{32}$$

Making the dimensionless coupling parameter independent of $N$ corresponds to making it impervious to a transformation that groups parts of the chain together, which characterizes the fixed point of the renormalization group method of decimation. For the unscreened Coulomb case, which gives $\nu = 2/(d - 2)$, the simplified procedure can be derived as a direct consequence of the decimation method, because charge is regarded as additive in the renormalization transformation.[18,48] The same result is also obtained by more advanced renormalization group treatments.[48,52] For excluded volume interactions, the connection to the decimation method[18] is less straightforward, but the result $\nu = 2/d$ is the one obtained, for example, by des Cloizeaux.[49,50]

Equations 24 and 32 represent two general classes of results. Bouchaud et al.[53] have studied the range of validity of different types of exponents. They found that in the regime $2 < \lambda < 4$, $\nu = 2/\lambda$ represents the behavior for a long-range potential, i.e., a potential that decays slowly compared to the dimensionality of the system. When the potential is short-range, the behavior is in the neighborhood of the Flory prediction for excluded volume effects; i.e., the behavior is described by $\nu_{SR} \approx 3/(d + 2)$. Furthermore, long-range is quantified as $\lambda < 2/\nu_{SR}$. For $\lambda < 1$, $\nu$ is given by the Flory formula. This has been confirmed by simulation in $d = 3$ for $\lambda = 2.5$ and $\lambda = 2$,[54] with the latter case requiring a logarithmic correction as predicted.[53]

*3.4.3. Excluded Volume Exponent.* For excluded volume interactions in three dimensions, the Flory exponent $\nu = 3/5$ is generally accepted as being very close to the correct value of $\nu$ for a self-avoiding walk, as indicated, for example, by lattice simulations.[46] On the other hand, $\nu = 2/\lambda$ gives $\nu = 2/3$ and this should be correct according to the criterium $\lambda = 3 < 2/\nu_{SR} = 10/3 \approx 3.33$.[53] There is not necessarily a contradiction, however. Bouchaud et al.[53] presented a heuristic argument showing how to recover the Flory value. A more direct explanation is that, while excluded volume interactions are often treated as $\lambda = d$, the interactions do not originate from a true $1/r^d$ potential. Self-exclusion on a lattice or hard-sphere interactions in continuous space have an instant decay and are thus extremely short-ranged, which would speak in favor of $\nu_{SR} = 3/5$. The situation may be less clear when the excluded volume treatment is used as an effective interaction replacing a softer potential.

There are also excluded volume treatments that give an interaction $U_{ev} \sim N/R$,[55,56] but are otherwise consistent with Flory theory and obtain $\nu = 2/3$ instead of the Flory value $\nu = 3/5$. This should not be confused with the results of the des Cloizeaux approach, which produces $\nu = 2/3$ from an excluded volume interaction corresponding to $U_{ev} \sim N^2/R^3$ in three dimensions (cf. eq 14).

The $\nu = 2/\lambda$ prediction for Coulomb interactions will be discussed in section 7.

## 4. Methods

**4.1. Monte Carlo Simulations.** Polyelectrolytes at infinite dilution, i.e., single chains, were simulated using the traditional Metropolis algorithm.[57] Two sets of models were used, both representing a polyion as a freely jointed chain with point charges that interact through the screened Coulomb potential, eq 1. All monomers have the same charge, $\alpha e$.

One model was used to reproduce the simulations of Micka and Kremer,[35] who applied a harmonic bond potential

$$u_{bond} = \frac{3k_BT}{2b^2} r_{i,i+1}^{\ 2} \tag{33}$$

where $r_{i,i+1}$ is the length of the bond between monomers $i$ and $i + 1$. In the absence of electrostatic interactions, the mean-square bond length would be $\langle r_{i,i+1}^{\ 2} \rangle = b^2$. In this model, $b$ and $\kappa^{-1}$ are expressed in units of Bjerrum length, since $l_B$ was set to 1 by Micka and Kremer.

In the other model, the bonds are rigid with a length $b$ expressed in Å. These simulations were performed with $T = 298$ K and a dielectric constant $\epsilon_r = 78.3$ corresponding to water at room temperature, which gives $l_B \approx 7.16$ Å. In this case, a chain labeled with a given number of monomers $N$ is actually the result of a simulation with a longer chain of length $N'$, but the interactions are truncated after $N$ monomers; i.e., monomers separated by $N$ bonds or more do not interact. This is to suppress end effects.[12] For $N = 160$, 320, 1000, and 3000, the maximum $N'$ was 1000, 2000, 5000, and 15000, respectively. A smaller $N'$ and even $N' = N$ can be used when the correlations die off within a lower number of bonds. The exception is $N = 5000$, which was only simulated with $N' = N$. Results are therefore not given for $\kappa = 0$ in this case. The dimensionless parameters that define the system are $\xi_p = \alpha^2 l_B/b$, $\kappa b$, and $N$.

The conformational sampling was performed with a pivot algorithm,[58,59] where trial conformations were obtained by dividing the chain into two parts around a bond. In the case of flexible bonds, one part was first translated as a whole and then rotated around one of the coordinate axes, chosen at random.[60] The translational displacement was randomly picked within a cubic box centered on the original position. The side of the box was 25 Å. The rotation angle was picked randomly within a full circle. With rigid bonds, only the rotation was performed and the rotation axis was a randomly chosen direction.[12,61]

Simulation lengths varied between $5 \times 10^6$ and $2.5 \times 10^8$ pivot moves. The longer simulations were used to get a high precision in the orientational correlation function for short screening lengths, where the correlation function is small and has a lower signal-to-noise ratio. The shorter simulations were used to keep the CPU time down for the longest chains, which still required about a CPU month for one simulation on a 1.1 GHz processor. To improve the precision in the latter case, the

orientational correlation function for bond separations up to one third of $N'$ was averaged over all possible pairs of bonds (for each bond separation) within the central third of the chain.

**4.2. Calculation of Projection Length.** For a discrete chain with rigid bonds, the projection length can be expressed as

$$l_p = \frac{1}{b}\langle \mathbf{r}_1 \cdot \mathbf{R}\rangle = \frac{1}{b}\sum_{j=1}^{N-1}\langle \mathbf{r}_1 \cdot \mathbf{r}_j\rangle = b\sum_{k=0}^{N-2}\langle \cos\theta_k\rangle \qquad (34)$$

where $\mathbf{r}_j$ is a bond vector, $\mathbf{R}$ is the end-to-end vector, and $\theta_k$ is an angle between bond vectors separated by $k$ bonds.

Although the projection length is conveniently defined as the projection of the end-to-end vector on the first bond, the first bond is unsuitable for simulation results, since it introduces end effects. Instead, the orientational correlation function $C_k \equiv \langle \cos\theta_k\rangle$ is calculated with respect to the central bond or as an average over the central part of the chain for longer chains.

Furthermore, the finite summation creates a trivial $N$ dependence when the correlations are long-ranged compared to the chain length. This jars with the idea of projection length as an intrinsic property (see next section) and is removed by extrapolating to $N \rightarrow \infty$ with the help of the snakelike chain, eq 9, fitted to the orientational correlation function. With end effects suppressed (translational invariance), the only $N$ dependence that is left is a direct result of the interactions, for example, the total number of charges in the unscreened case and excluded volume effects in the screened case.

Finally, $l_p$ in the absence of electrostatic interactions is $b$, since the chain is then freely jointed. This contribution is subtracted to yield the electrostatic projection length, $l_{p,e} = l_p - b$.

## 5. Simulation Results

Since the end-to-end distance and the projection length are closely related ($\langle R^2\rangle = 2Ll_p$ for very long chains), there is a choice between studying one or the other. I will focus on projection length for practical and conceptual reasons. One of the best ways to understand the conformational behavior is through the orientational correlation function. The projection length is the integral over this function. Simulations necessarily deal with finite chains and these may not be long enough to allow the correlations to die off completely over a range comparable to the contour length $L$, but the integral is easily extrapolated to infinite chain length with the help of the two parameters of the snakelike model, eq 9. This infinite-chain projection length can be viewed as an intrinsic property of the chain, independent of chain size (given that the range of interactions is finite). End-to-end distance, on the other hand, is always coupled to chain length and its relation to the orientational correlation function is more complicated. Given the orientational correlation function and the snakelike chain, the mean-square end-to-end distance can be calculated for any chain length (beyond the short-range flexibility),

$$\langle R^2\rangle = 2\int_0^L (L-s)C(s)\,\mathrm{d}s = 2C_0 l_{oc}[L - l_{oc}(1 - \mathrm{e}^{-L/l_{oc}})] \qquad (35)$$

**5.1. Three Regimes.** When not too long chains are simulated, two regimes can be observed in the behavior of the projection length and both can be described by power laws. In the salt-free limit, the projection length is, obviously, independent of $\kappa$ and remains approximately so at low concentrations of salt, until the screening length becomes comparable to the chain dimensions. For the model that suppresses end effects, the following empirical expression has been obtained:[12]

$$\frac{l_p}{b} \approx A\xi_p N^2 \qquad (36)$$

with the numerical constant $A \approx 0.04$. This is qualitatively the same as eq 6, which follows from Odijk's expression, eq 3. The corresponding power law at high salt concentrations was

$$\frac{l_{p,e}}{b} \approx B\left(\frac{\xi_p^{1/2}}{\kappa b}\right)^{1.2} N^{0.3} \qquad (37)$$

with the numerical constant $B \approx 0.8$. By combining the two power laws, the simulation results were shown to fall onto a universal curve over a wide range of $\xi_p$, $\kappa b$, and $N$.[12] Note that these three dimensionless parameters specify the system completely. The latter power law, eq 37, contains a close to linear dependence on the screening length, which is the result usually reported for the projection length in simulations.[12,14,27,29]

For longer chains, a third, intermediate regime appears.[12,36,37] All three regimes are shown in Figure 1a, where the behavior in the intermediate regime can be represented as

$$\frac{l_{p,e}}{b} \sim \left(\frac{\xi_p^{1/2}}{\kappa b}\right)^{1.8} \qquad (38)$$

which is close to the asymptotic OSF result, eq 5.

Three regimes are also suggested by a consideration of the relation between the screening length and chain size. When $\kappa^{-1}$ is much larger than the chain dimensions, the chain is effectively unscreened, which means that all monomers interact and the projection length should be strongly dependent on $N$. If the electrostatic interactions are strong and numerous enough, the chain is expected to be rodlike. When $\kappa^{-1}$ becomes comparable to the chain size, the conformational behavior will start to depend on the screening length. As long as the chain remains stiff or semiflexible, the screened electrostatic interactions will be localized to sequential sections, which are kept apart by the stiffness. Thus, correlations will have a finite range, which means that the projection length will be independent of $N$ and the orientational correlation function will have an exponential decay. This will be referred to as the Debye−Hückel (DH) regime. When the salt concentration is high and the screening length is short compared to the chain length, there is a non-negligible probability that the chain will loop back on itself and allow distant parts to interact occasionally. In other words, so-called excluded volume effects should become important and there should be a weak dependence on $N$. The orientational correlation function will decay more slowly than exponentially and this will be used as the definition of an excluded volume regime.

These considerations and the expected dependence on $N$ are consistent with the observed behavior, eqs 36−38. Also the fact that the intermediate regime, i.e., the DH regime, is only observed for long chains may be anticipated. An extended DH regime requires that the projection length is much longer than the screening length, to allow a large range of screening lengths where the chain is semiflexible. A short or weakly charged chain may not have much of an opportunity to gather enough stiffness before the screening length outgrows the chain dimensions and the unscreened regime begins.

**5.2. Comparison with Theory.** The notion of three regimes is also the basis for the scaling laws described in section 3.4.1, and with $R^2 \approx 2Ll_p$, we see that the set, eqs 16−18, that is based on the OSFKK picture is quite close to the simulation

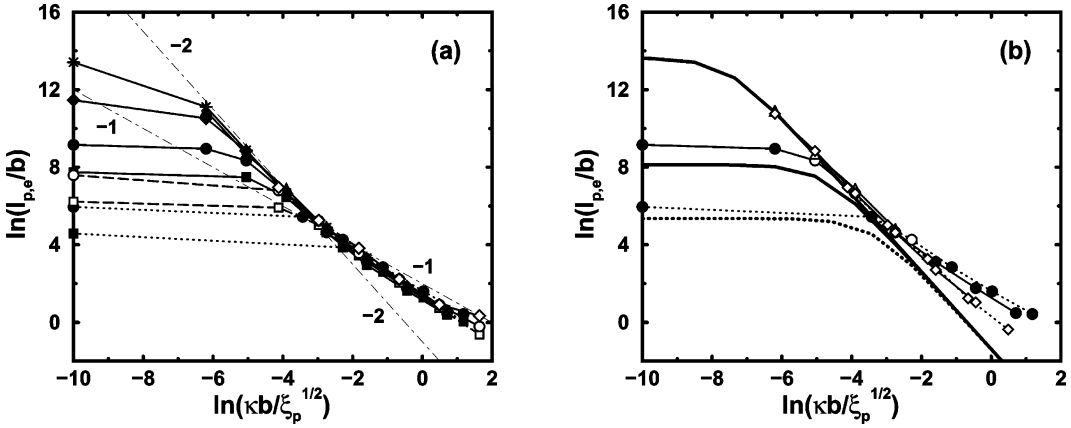


**Figure 1.** The behavior of the electrostatic projection length as a function of $\kappa b/\xi_p^{1/2}$. (a) Simulation results for $\xi_p = 2.4$ ($b = 3$ Å and $\alpha = 1$) (filled symbols and solid lines) with $N = 160$ (squares), 320 (circles), 1000 (diamonds), 3000 (stars), and 5000 (triangles); $\xi_p = 0.60$ ($b = 12$ Å and $\alpha = 1$) (open symbols and dashed lines) with $N = 160-1000$; and $\xi_p = 0.15$ ($b = 12$ Å and $\alpha = 0.5$) (filled symbols and dotted lines) with $N = 160-320$. Points on the *y*-axis represent the salt-free case ($\kappa = 0$). Otherwise the dimensionless screening length $(\kappa b)^{-1}$ ranges from 320 down to 0.25 bonds (from left to right). The dot−dashed lines are guides to the eye with slopes as indicated. (b) Simulation results for $\xi_p = 2.4$ (thin solid lines) with $N = 320$ (circles) and 5000 (triangles) as well as $\xi_p = 0.15$ (thin dotted lines) with $N = 320$ are compared to the corresponding predictions of the Odijk expression, eq 3, (thick lines without symbols). Here open symbols (mostly hidden under diamonds) represent the points deemed to be in the DH regime and the diamonds denote a generalized DH regime, obtained by selecting chain lengths unaffected by excluded volume interactions (see text).

result. In particular, the asymptotic behavior that follows from the excluded volume treatment of Odijk and Houwaart (OH)[45] leads to $l_p \sim \kappa^{-6/5}$ (cf. eq 18),[16,19,36,37] which happens to be the same as the simulation result $l_p \sim \kappa^{-1.2}$ of eq 37. Thus, it would appear that the OSFKK picture is essentially correct and that the apparent disagreement with OSFKK (screening-length exponent of 2) observed in simulations and experiments (exponent close to 1) may be due to excluded volume effects. This is corroborated by the fact that excluded volume effects have been demonstrated to be significant at the highest salt concentrations.[12]

Figure 1b explores the idea that the Odijk expression, eq 3, is qualitatively correct up to a point where excluded volume effects become significant. The expression predicts a bending coefficient rather than a projection length and eq 3 underestimates the latter in the salt-free limit, but the general trends are in agreement with simulations for the unscreened and DH regimes. The DH regime may be characterized by points that neither tend to the asymptotic salt-free limit nor show any *N* dependence as a result of excluded volume effects. Thus, when simulated points seem to fall onto a universal curve independent of chain length, this has been taken to indicate that they belong to the DH regime. For $N = 320$ and 5000 plotted in Figure 1b, such points have been found in the range $-6.2 < \ln(\kappa b/\xi_p^{1/2}) < -2.7$ and are marked by open circles and triangles, respectively (mostly hidden by diamonds). This is a very subjective measure of the DH regime, but it does roughly coincide with the region where the simulations are in fair agreement with the screened limit ($l_p \sim \kappa^{-2}$) of Odijk's expression.

It is generally accepted that OSF theory can be applied to stiff chains. The controversial issue has been whether it holds for flexible chains. The success of eq 18 seems to imply that it does, if it is supplemented by an excluded volume treatment. This idea has also been pursued in a series of papers by Reed and Reed,[27,62,63] who compared simulation results to various treatments of electrostatic excluded volume starting from the ideas of Odijk and Houwaart.[45] However, the agreement with simulation was only fair at best, although a great improvement over OSF theory alone. Comparisons between experimental

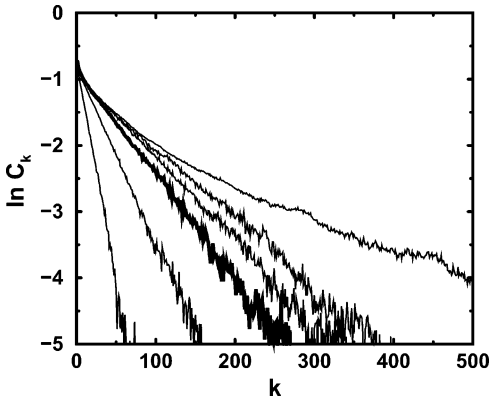


**Figure 2.** Logarithmic plot of the orientational correlation function for chains with $b = 12$ Å, $\alpha = 1$, $\kappa^{-1} = 30$ Å, and $N = 5000$, 320, 160, 80, 40, 20 (top to bottom). For $N \leq 320$, *N* represents the range of interactions in chains with $N' = 1000$ monomers. The thick line shows the chain length, $N = 80$, chosen to represent the generalized DH regime for this screening length (see the text).

results and excluded volume theories following OH show the same trends as the comparisons with simulations.[27,31,32,34] It is interesting to note that Sorci and Reed[34] found a relation between the squared radius of gyration and the concentration of added 1:1 salt $\langle R_G^2 \rangle \propto c_s^{-0.609}$, which, with $\kappa^2 \propto c_s$, also gives an effective exponent of 1.2 for the screening length as in eq 18. Apparently the simple asymptotic prediction, represented by eq 18, is able to reproduce both simulated and experimental results surprisingly well, while the more advanced excluded volume treatments still leave a few things to be desired.

Let us now test the idea that the chain should show OSFKK behavior if the excluded volume effects were removed, as suggested by the excluded volume treatments that follow from OH. The excluded volume effects are manifested as a slower than exponential decay of the orientational correlation function $C_k$ at large bond separations *k*. In a plot of ln $C_k$ vs *k*, this corresponds to a deviation from a linear behavior. The effect is illustrated in Figure 2 for different chain lengths, where *N* represents a truncation of the interactions in a simulation of a longer chain.

In the model with truncated interactions, ln $C_k$ vs $k$ always becomes linear for $k > N$ since, after the truncation, correlations can only be transmitted through the chain, which automatically produces an exponentially decaying correlation function.[64] If the chain is not too flexible, there is also a linear regime right after the initial decay due to the short-range flexibility. This represents the behavior before excluded volume effects set in and is the same for all $N$ larger than some value $N_0$, which marks the point where the screened electrostatics have decayed sufficiently before they are truncated. Results free from excluded volume effects can be obtained by choosing $N$ for each $\kappa$ so that the long-range linear behavior is consistent with the short-range linear behavior seen also for longer chains ($N > N_0$).

The diamonds of Figure 1b represent this type of generalized DH regime for two values of the coupling parameter $\xi_p$. In the intermediate, semiflexible regime, the chains are already in a DH regime and the selection of points does not change the result, i.e., $l_p \sim \kappa^{-1.8}$. We will therefore focus on the generalized DH behavior in the regime where excluded volume effects are seen for the longer chains. Here, the result is $l_p \sim \kappa^{-1.6}$. Although the exponent for the screening length is no longer close to 1, it is not quite OSFKK-like either. Once again, the choice of data points is subjective. To test the uncertainty, consistently smaller as well as larger $N$ were tried and the error bars were estimated to be $1.6 \pm 0.1$. This value should not be taken as a new "magic" exponent. The point is that it is not expected to get much closer to 2.

In other words, in the flexible regime, the generalized DH regime is not exactly OSFKK-like, which undermines the excluded volume treatment based on the ideas of OH with $l_p \sim \kappa^{-2}$. This may explain why the simple scaling law eq 18 does a decent job, while a more advanced excluded volume treatment has had a rather limited success.[27,62,63] It is a common observation that a crude first-order approximation gets close to the mark thanks to a substantial cancellation of errors, while an "improvement" to the theory fails, because it only reduces some of the errors. The prediction of $\nu = 3/5$ for a self-avoiding walk by the simple Flory approach is another typical example.

Furthermore, a difficulty arises for the shortest screening lengths, where the chains are also most flexible. Here, excluded volume effects become apparent on length scales comparable to the initial short-range decay and it becomes hard to tell where "short-range" ends and "long-range" begins, if such a distinction is even meaningful. It is also telling that the chain length chosen to represent the generalized DH regime for the shortest screening length and the weakest coupling is $N = 9$, which can hardly be said to represent a *poly*electrolyte. All interactions are screened Coulomb interactions and it no longer makes much sense to divide them into short-range, sequential ones producing an effective stiffness and long-range "excluded volume effects". The loss of a persistent range, i.e., the formation of a regime where a short-range flexibility goes directly over into a long-range swollen behavior without an intermediate stiffness has also been discussed by Netz and Orland.[22]

A more direct interpretation of the close to linear dependence of the persistence length on the screening length observed in simulations and experiments has been offered by variational calculations,[17,21,25,26] but this is predicted in the absence of excluded volume effects. Inclusion of this effect in a scaling treatment leads to a sublinear dependence on the screening length, $l_p \sim \kappa^{-4/5}$ (cf. eq 21),[19,36,37] which is not in agreement with simulations. Another objection against the scaling result, eqs 19−21, follows from a crossover analysis that shows that the intermediate regime should not be observed,[36,37] while it does appear for long chains in simulations. This is a weaker argument, because the observation of the intermediate regime could be interpreted as a change of behavior to OSFKK-like when there is enough electrostatic interactions to make the chains rather stiff. A more comprehensive set of arguments has been presented by Everaers et al.,[36] who concluded that the linear prediction in the form of the scaling laws, eqs 19−21, can be ruled out.

**5.3. Summary.** Long chains display three regimes: an unscreened regime, a DH regime, and an excluded volume regime. The electrostatic projection length can be described by power laws in these regimes.

The Odijk expression, eq 3, is qualitatively correct as long as the chains are rather stiff, due to strong, long-range electrostatic interactions. A similar stiffening can also be achieved by a bond-angle potential.[13,14]

A close to linear dependence of the projection length on the screening length is associated with excluded volume effects, which are seen as a slower than exponential decay of the orientational correlation function. However, an OSFKK-type behavior is not observed when the excluded volume effects are removed, as suggested by the predictions that build on OSF theory and the ideas of Odijk and Houwaart.

The linear prediction obtained by variational calculations in the absence of excluded volume effects does not offer a good description of the system.

## 6. Variational and Perturbational Results

Many different variational calculations predict $l_p \sim \kappa^{-1}$ without excluded volume interactions.[17,21,25,26] What do they have in common and where do they deviate from the simulation results? In other cases, analytical theories have produced OSFKK behavior, $l_p \sim \kappa^{-2}$.[7,8,20−24] What are the differences? These are the questions that will be answered next.

**6.1. Method Dependence.** Ha and Thirumalai[21] (HT) have suggested that differences between the Edwards−Singh (ES) method,[65] which they used, and the more commonly used Gibbs−Bogoliubov (GB) approach can sometimes cause different scaling results (introductions to the two methods can also be found in refs 10, 26, 66). This was based on the observation that they obtained $l_p \sim \kappa^{-2}$ with the ES method, while Barrat and Joanny[17] (BJ) found $l_p \sim \kappa^{-1}$ through the GB approach, when starting from the same variational model. However, the analysis of BJ was not a systematic application of the full Hamiltonian and the two groups employed different additional approximations (see below). Thus, the comparison does not really say much about differences between the ES and GB methods.

To strengthen the argument and demonstrate a limitation of the GB approach, HT also supplied an example in an appendix. This consisted of a bending model with a Fourier transformed kernel, $K_q = l_0 + \kappa^2 l_{OSF}/(\kappa^2 + 2q^2)$, where $l_{OSF} = l_B/(4\kappa^2 A^2)$ and $A$ is the distance between unit charges. Using the trial kernel $\tilde{K}_q = l_p$ (independent if the reciprocal length $q$), the GB approach was shown to yield $l_p \sim l_0 + \Lambda l_B/(\kappa A^2)$, where $\Lambda^{-1}$ is the upper bound for $q$, while the ES method gave $l_p \approx l_0 + l_{OSF} = l_0 + l_B/(4\kappa^2 A^2)$. However, the two calculations were not entirely consistent with each other, because the former involved an explicit summation over $q$ before the free energy was minimized, while it was argued in the latter that $q \approx 0$ would give a dominating contribution.

If the variational free energy in the GB calculation is minimized first and optimized for each $q$ value separately, the

result is (cf. eqs B5 and B6 of ref 21)

$$l_p = l_0 + \frac{\kappa^2}{\kappa^2 + 2q^2} l_{OSF} \tag{39}$$

which also gives $l_p = l_0 + l_{OSF}$ when $q = 0$. In other words, both methods give the correct result for $q = 0$ when no other value of $q$ is taken into account. Obviously, a $q$-independent kernel cannot exactly reproduce a $q$-dependent one and a compromise is necessary when all $q$ values are considered at the same time. Hence, the deviating "GB" result. This illustrates a completely different point, namely that there is a problem when there is a scale dependence and only one (scale independent) variational parameter.

To conclude the discussion about the GB and ES approaches, I would like to point out that the two methods are quite similar. With a variational parameter $a$, both formally correspond to solving the equation

$$\langle X(H - H_0)\rangle_0 - \langle X\rangle_0 \langle H - H_0\rangle_0 = 0 \tag{40}$$

where $H$ is the Hamiltonian of the model, $H_0$ is the trial Hamiltonian and $\langle ... \rangle_0$ is an average with respect to the trial system. $X \equiv dH_0/da$ in the GB approach, while in the ES method, $X$ is any property that should be optimized, which, in this context, means $X \equiv R^2$ (or $X \equiv \theta^2(L)$, in the example of HT (see appendix B of ref 21), where $\theta^2(L)$ is the square of the angle between the directions of the chain ends). If the trial Hamiltonian can be written $H_0 = f(a)R^2$, with $f(a)$ being a function of $a$, independent of the chain conformation, the two methods are equivalent. The differences that do exist with other trial Hamiltonians cannot explain the general observation of the two types of results, since both OSFKK and the linear prediction can be obtained via either method. Indeed, HT[21,26] themselves have obtained both results using the ES method, the difference being the use of two-parameter and one-parameter models, respectively (see below).

**6.2. Model Dependence.** More important for the outcome of a variational calculation are the approximations involved. To obtain a simple answer from an analytical approach, simplifications are generally needed, either in the initial ansatz, along the way, or by taking the result to an asymptotic limit, or even all of the above. Many approaches use only a single parameter to represent the conformational behavior. This generally leaves a choice between mapping the behavior onto an unperturbed chain or making a perturbative expansion around a rodlike state. The former emphasizes flexibility, with $l_p \sim \kappa^{-1}$ as the usual result, while the latter, starting from rigidity, is identical to OSF theory, if the persistence length is identified with an effective bending coefficient.

As we know from simulations, the orientational correlation function of a charged chain has a fast short-range decay and a slower long-range decay. The fact that a chain can have both short-range flexibility and a stiffer long-range behavior forms the basis of the blob picture and it also follows from the theoretical analysis of Li and Witten.[20] A single parameter cannot handle the two types of behavior at the same time.

One-parameter models using the Gaussian statistics of an unperturbed chain can at best describe the short-range flexibility. The Flory approach (without any help from OSF theory), which is based on the freely jointed chain, is the archetype of such models. A close relative is an ansatz where the variational Hamiltonian is just a freely jointed chain with harmonic bonds, as in the theory of Muthukumar[5,6] and one of the models used by Ha and Thirumalai.[21] This corresponds to having eq 33 as the bond potential and using $b$ as the variational parameter. The short-range nature of the result using this Hamiltonian is rather obvious, considering that the variational parameter corresponds to an average bond length and that the Hamiltonian does not contain a description of long-range correlations. In fact, a freely jointed chain, by definition, does not have any correlations beyond a bond. These models give either $l_p \sim \kappa^{-0.8}$ or $l_p \sim \kappa^{-1}$, depending on whether excluded volume interactions are included or not (cf. eqs 21 and 20).

The $l_p \sim \kappa^{-1}$ behavior has also been obtained by Ha and Thirumalai[26] and Schmidt[25] based on the wormlike-chain model. HT used the model of Lagowski, Noolandi, and Nickel[67] (also used by Muthukumar and co-workers in ref 68), which is actually a hybrid between a Gaussian and a wormlike chain. Schmidt used the wormlike-chain model to calculate the electrostatic energy and the end-to-end distance in a Gaussian entropy term in an approach similar to that of Katchalsky and Lifson,[4] who employed a freely jointed chain. Once again, these models rely on a single variational parameter.

OSF theory is also based on a one-parameter model, but, unlike the models just discussed, the theory introduces long-range correlations from the start by considering deviations from a perfectly rodlike state. Another difference is that the electrostatic persistence length is calculated directly via the electrostatic cost of bending the rod slightly, expressed as a function of the deformation, as opposed to determining the average deformation variationally by solving an equation like eq 40. Li and Witten[20] have done the separation of length scales more explicitly by considering the different modes of deformation of a ring and calculating the bending coefficient of the long-range fluctuations, which is equivalent to OSF theory. It is also possible to obtain OSF theory as a part of a $1/d$-expansion.[23,24]

A wormlike chain is a one-parameter model, but a reasonable description of the chain behavior can be obtained by introducing an additional parameter that handles the short-range flexibility, as in the snakelike chain, eq 9. The point is that more parameters allow a separation of the behavior on different length scales. Such a separation is most obvious in the blob model,[15,16] where the chain behavior is treated on two levels. Inside a blob, the chain is unperturbed, which determines the blob size, and on a coarse-grained level, the chain is seen as a chain of blobs. Khokhlov and Khachaturian[16] applied OSF theory directly to the blob model.

The same type of coarse graining is possible with the tension-field model of Barrat and Joanny.[17] This model has two parameters and is congruent with the snakelike chain.[12,14] When Ha and Thirumalai[21] applied the tension-field model, they obtained a result very similar to that of KK for the effective (coarse-grained) persistence length, which, in terms of the snakelike chain, is $\sqrt{C_0} l_{oc}$ and represents the orientational correlation length of an underlying wormlike chain.[12] Note that the projection length discussed in connection with the simulations above corresponds to $C_0 l_{oc}$.

The variational calculation performed by BJ themselves was based on the idea of the tension-field model, but the problem was reformulated in terms of the blob picture with separate arguments for separate terms in the Hamiltonian. This lead to a separation of parameters into different terms and the minimization with respect to $l_p$, in effect, corresponded to the optimization of a one-parameter model, representing the chain of blobs. Furthermore, this chain was treated as an unperturbed (wormlike) chain, which resulted in $l_p \sim \kappa^{-1}$.

As mentioned above, HT started out by using the method of Edwards and Singh, but also reverted to a blob picture to

simplify the calculations. In contrast to BJ, they only considered the stiff part of the blob chain and represented it as a rod in the integral containing the electrostatic interactions. More importantly, the approximations made the integral independent of $l_p$ and since $l_p$ is equal to this integral, $l_p$ was calculated directly rather than being determined self-consistently. Thus, the treatment of HT has more in common with the perturbative calculation of OSF than a variational calculation for a flexible chain. It is then not surprising that they obtained the OSFKK result.

**6.3. Parameter Reduction.** The crossover distances, $l_{cd}$, that follow from the respective analyses of Bratko and Dawson[51] (BD) and Netz and Orland[22] (NO) illustrate how a more general approach can be deflated to a simple Flory-type level and also lead to different results by the stroke of just a few additional approximations. The short version is that BD and NO started from the same general Gaussian ansatz and treated the screened electrostatics in a form equivalent to a pure excluded volume effect, but BD consciously directed the results to yield a Flory-type swollen behavior, $\langle R^2\rangle \sim N^{6/5}$, while NO used the arguments of des Cloizeaux[49,50] to obtain $\langle R^2\rangle \sim N^{4/3}$. This leads to $l_{cd} \sim \kappa^{-1}$ and $l_{cd} \sim \kappa^{-2}$, respectively.[10] To be exact, NO also considered estimates of an effective, short-range stiffness, which allowed for the intrinsic flexibility on even shorter length scales and produced corrections (mainly logarithmic) to the $\kappa$ dependence, but if the effective stiffness is taken to be independent of $\kappa$, the pure $l_{cd} \sim \kappa^{-2}$ is obtained.

The general Gaussian ansatz has a separate parameter $b(n)$ for each value of $n$, where $b(n)$ represents the mean-square end-to-end distance $\langle R^2(n)\rangle$ of a subchain with $n$ bonds. However, des Cloizeaux, BD, and NO, applied the additional ansatz that $b(n) \sim b_0 n^{2\nu}$, where $b_0$ is a constant, thus reducing the number of parameters to two. Furthermore, the variational equation was expressed in Fourier space, where the parameter set corresponding to $b(n)$ is $g^{-1}(k)$, which, with the additional ansatz, becomes $g(k) = g_0 k^{1+2\nu}$. Apart from the excluded volume interactions, the model had harmonic bonds, eq 33, which in Fourier space and in the small $k$ limit corresponds to a term $3k^2/2b^2$ in the variational expression. The quadratic dependence on $k$ is typical of a Gaussian behavior, which gives $\nu = 1/2$, and appears here because the Boltzmann weight of a harmonic bond, $\exp(-3r_{i,i+1}^2/2b^2)$, is Gaussian.

The excluded volume interaction can be expanded to give two terms with $k$ dependences $k^2$ and $k^{\nu(d+2)-1}$, respectively,[49,50] where $d$ is the spatial dimension. Des Cloizeaux suggested that the first term should cancel the bond term, which is also of order $k^2$, and the second should be balanced with a remaining free energy term, which is of order $k^{1+2\nu}$. Matching of the orders $\nu(d+2) - 1 = 1 + 2\nu$ gives $\nu = 2/d$. BD, on the other hand, argued that the $k^2$ part of the excluded volume expansion is unphysical and corresponds to short-ranged excluded volume interactions. BD simply dropped the term and said that the dominating balance should be between the second excluded volume term and the bond term, which means that $\nu(d+2) - 1 = 2$; i.e., the exponent has the Flory-type value $\nu = 3/(d+2)$. The treatment of des Cloizeaux has also been criticized by Migliorini et al.[69] on the grounds that it introduces extra restrictions and that the expansion used is only valid for noninteger values of $\nu(d+2)$, which is an integer if $\nu = 3/(d+2)$ is the preferred value. Like BD, Migliorini et al. set up a balance with the bond term to enforce the Flory-type swelling behavior, but their expansion for integer $\nu(d+2)$ also introduces logarithmic corrections. As discussed in section 3.4.2, there is also support,[53,54] within certain limits, for the general class of results that the des Cloizeaux analysis belongs to, but it is questionable in the case of excluded volume interactions that are not the result of a true $1/r^d$ potential.

The BD approach produces the Flory exponent $\nu = 3/5$ and the behavior of eq 21, because it contains the same elements as a simple Flory analysis, namely an interaction term balanced against a Gaussian term. In fact, the matching of powers described above can be mapped onto the procedure represented by eqs 25−28. There is a difference, however. In the Flory approach, the Gaussian term represents the entropy of a freely jointed chain, while the BD term originates from the harmonic bond potential, eq 33. Still, the difference disappears, if $b$ in the bond potential is reinterpreted as the actual bond length or Kuhn length and not just the unperturbed value.

Although the analysis of Netz and Orland produced an OSFKK-type result, $l_{cd} \sim \kappa^{-2}$, it differs from the set represented by eqs 16−18, because the predicted swollen behavior was

$$\langle R^2\rangle \sim \frac{\alpha^{4/3} l_B^{\,2/3} N^{4/3}}{\kappa^{4/3}} \tag{41}$$

which belongs to the class represented by eq 32. Note that eq 18 was based on a rodlike excluded volume and an explicit use of OSF theory, while NO (and BD) had a spherical volume $V_e \sim \alpha^2 l_B/\kappa^2$ without extra assumptions. The crossover distance of NO becomes OSFKK-like as a result of combining the usual rodlike description for the short-range (unscreened) behavior with the des Cloizeaux prescription for the long-range (screened) part. The latter represents a stiffer swollen behavior, $\nu = 2/3$, compared to the Flory value $\nu = 3/5$. As mentioned above, NO obtained alternative expressions for the crossover distance by considering different types of ($\kappa$ dependent) short-range behavior.

While simulations[12] give $l_p \sim \kappa^{-1.2}$ as in eq 18, they cannot be said to exclude $l_p \sim \kappa^{-1.33}$ of eq 41. Neither are they conclusive regarding $\nu = 3/5$ or $\nu = 2/3$ as the swelling exponent. $N^{0.3}$ in eq 37 for the projection length implies $\nu \approx 1.3/2 = 0.65$, but a direct calculation of the end-to-end distance gave $\nu \approx 1.1/2 = 0.55$.[12] Still, $\nu = 3/5$ is expected to be a better estimate for the swollen behavior than $\nu = 2/3$ on the grounds that the Flory exponent describes a self-avoiding walk very well and the screened Coulomb potential $\exp(-\kappa r)/r$ is more short-ranged than the electrostatic excluded volume potential $1/(\kappa^2 r^3)$ (cf. section 3.4.3). Thus, as a first approximation, eq 18 would be preferred over eq 41.

**6.4. Numerical Results.** A truly general Gaussian ansatz has been solved numerically and the results have been compared with simulations.[14,66,70,71] The approach shows good agreement for the end-to-end distance in the unscreened case and can also reproduce orientational correlation functions.[66] In the screened case, however, the end-to-end distance is consistently overestimated, because the Gaussian Boltzmann distribution overestimates the interaction.[71] Expressed as an electrostatic projection length, the variational results have displayed similar trends as the simulation results also in the screened regime,[14] but this was for a chain length where the simulated chains are influenced by excluded volume effects. Such effects produce an apparent, qualitative agreement also with less general Gaussian approximations that neglect excluded volume interactions. Further studies are needed to evaluate the general ansatz more fully.

**6.5. Summary.** The majority of analytical approaches belong to one of two kinds. The linear prediction or scaling according to eqs 19−21 is typical of a trial system with a high degree of flexibility represented by Gaussian statistics and a single

variational parameter. This corresponds at best to the short-range flexibility seen in polyelectrolytes and may describe local stretching of the chain. OSF theory represents a perturbation around a rigid state and deals explicitly with a long-range bending mode.

Both approaches make the assumption that there is a single behavior that describes the chain on all length scales. This is not correct for a flexible polyelectrolyte. With more than one variational parameter, short-range flexibility and long-range stiffness can be handled simultaneously. The simplest form is the blob picture, where the short-range behavior is represented by the blob size and the coarse-grained chain of blobs is treated as a normal one-parameter model, but the blob size is usually taken for granted and nothing is gained. For example, the tension-field model of Barrat and Joanny[17] allows a reformulation in terms of blobs and have lead to both the linear prediction and OSFKK behavior, depending on the type of approximation used to describe the chain of blobs. More general approaches have also been brought down to the level of a one-parameter model by the assumption that there is a single behavior on all length scales.

Li and Witten[20] have analyzed differences in the behavior on different length scales, but it is still unclear whether a truly general variational (Gaussian) ansatz will reproduce the same length-scale dependence as seen in simulations.

### 7. Field-Theoretic Renormalization Group Analysis

Liverpool and Stapper (LS) have applied a field-theoretic renormalization group analysis to a Gaussian chain with screened Coulomb interactions.[38,39] They focused on the Debye−Hückel regime, where the screened Coulomb interactions are significant; i.e., the screening length $\kappa^{-1}$ is neither much longer than the chain, which would make the chain unscreened and rodlike, nor very short, which would turn the electrostatic interactions into short-ranged excluded volume interactions. The analysis was restricted to weakly charged polyelectrolytes, whose local structure is unaffected by the electrostatic interactions, i.e., remains Gaussian.

**7.1. Full Treatment.** The polymer and the screened Coulomb interactions were represented as two independent fields, which means that there were two sets of critical exponents, $(\nu_p,\eta_p)$ and $(\nu_C,\eta_C)$, respectively. The polymer exponents were the same as obtained for the unscreened case ($\kappa = 0$) and $\nu_p$ corresponds to the exponent $\nu$ of $\langle R^2\rangle \sim N^{2\nu}$ for the unscreened chain. Renormalization group methods give $\nu_p = 2/(d-2)$ (see also section 3.4.2).[48,52] However, this result applies at most to the spatial dimensions $4 \le d \le 6$. In three-dimensional space ($d = 3$), $\nu_p = 2$, but $\nu$ cannot be larger than 1, which corresponds to a fully stretched chain (rod). Thus, the behavior of the chain is expected to change and stay rodlike ($\nu_p = 1$) for $d \le 4$. The change has been explained as the fixed point of the renormalization group transformation becoming unstable at $d < 4$[48] and in terms of swelling corrections that become important and have to be included below an undetermined dimension $d^* < 6$.[72,73] A more direct illustration has been given by de Gennes.[18]

A simple Flory argument leads to $\nu_p = 3/d$,[15,48] which directly gives $\nu_p = 1$ for $d = 3$. Baumgärtner[74] has found excellent agreement between the Flory result and simulations for $3 \le d \le 6$, while, consequently, the renormalization group exponent did not fit the simulation data for $d < 6$. Thus, this result would indicate that the limiting dimension $d^*$ is close to 6.

Liverpool and Stapper argued that $\nu_p = 2/(d-2)$ is valid also in three dimensions when the screening length is comparable to the chain size, or, actually, that it is in this regime that result is obtained and not in the limit where $\kappa \to 0$, while $N$ remains finite.[38] The swelling corrections discussed by Jug[72,73] were considered to be corrections also to the DH model and, thus, $\nu_p = 2/(d-2)$ was said to remain valid at $d < 4$ for the pure, uncorrected DH case.[38]

LS found[38,39]

$$\langle R^2\rangle \sim \frac{(\kappa b)^{1/\nu_p} N}{\kappa^2} f((\kappa b)^{1/\nu_p} N) \tag{42}$$

where $b$ is the Kuhn length and $N$ the number of Kuhn segments. Explicitly in three dimensions, this becomes

$$\langle R^2\rangle \sim \frac{(\kappa b)^{1/2} N}{\kappa^2} f((\kappa b)^{1/2} N) \tag{43}$$

One of the main results of this is that $(\kappa b)^{1/\nu_p}N$ is identified as the proper scaling variable and the DH regime is characterized as $(\kappa b)^{1/\nu_p}N \sim 1$.[39] With $d = 3$, this is inconsistent and actually corresponds to the unscreened regime, since $(\kappa b)^{1/2}N \sim 1$ implies $\kappa b N \sim 1/N$; i.e., for long chains, the screening length is much longer than the fully stretched chain.

In the letter,[38] LS used the comparison between the screening length and the unperturbed dimensions of the chain, $(\kappa b)^2 N \sim 1$, to define the DH regime. This would be the obvious choice as long as the chain is not extended, since, logically, the DH regime corresponds to $b^2 \ll \kappa^{-2} \ll \langle R^2\rangle$. Using $(\kappa b)^2 N \sim 1$ to eliminate $\kappa$ in eq 42 gives

$$\langle R^2\rangle \sim b^2 N^{2-1/(2\nu_p)} f((\kappa b)^{1/\nu_p} N) \tag{44}$$

An effective exponent $\nu_{eff} = 1 - 1/(4\nu_p)$ is obtained, given only a weak $N$ dependence through $f((\kappa b)^{1/\nu_p}N)$. With $d = 3$, $\nu_{eff} = 7/8$, which corresponds to a rather extended, but not overextended, chain. This was presented as proof that the theory using $\nu_p = 2/(d-2)$ should be valid also in three dimensions,[38] although there is an apparent inconsistency between $\nu_{eff} = 7/8$ (extended chain) and $\nu = 1/2$ (unperturbed chain) implied in $(\kappa b)^2 N \sim 1$.

However, the correct DH fixed point consistent with the theory is $(\kappa b)^{1/\nu_p}N \sim 1$,[75] as used in their subsequent paper.[39] Using this to eliminate $\kappa$ leads to

$$\langle R^2\rangle \sim b^{1/2} N^{1+3\nu_p/2} f((\kappa b)^{1/\nu_p} N) \tag{45}$$

and $\nu_{eff} = 1/2 + 3\nu_p/4$. In three dimensions, $\nu_{eff} = 2$, which is numerically the same as $\nu_p$ and corresponds to an impossible overstretching.

On the basis of the nontrivial character of $f(x)$, evaluated to first order in $\epsilon = 6 - d$, LS suggested that a simple power law should not exist for $\langle R^2\rangle$ in the DH regime. To prove the point, LS plotted the approximate $f(x)$ around $x = 1$ with $d = 3$,[39] but as just discussed, $(\kappa b)^{1/\nu_p}N \sim 1$ with $\nu_p = 2/(d-2)$ corresponds to the rodlike rather than the DH regime in the three-dimensional case and, furthermore, implies overstretching. In other words, this numerical evaluation around $f(1)$ does not have any general significance.

Moreover, the analysis of $f(x)$ is of little consequence, if eq 42 is not a good general expression. To show that it applies to $d = 3$, LS[38] set out to make a log−log plot of $(\langle R^2\rangle\kappa^2/(\kappa b)^{1/2}N)^{1/2}$ vs $(\kappa b)^{1/2}N$ (rescaled for each bond length to remove multiplicative constants, which depend on $b$, but not on $\kappa$ and $N$[75]) using simulation data of Micka and Kremer[35] (MK). According to eq 43, all the points should fall onto a universal curve representing $f(x)$ (literally $\log f^{1/2}(x)$ vs $\log x$), which indeed they appeared

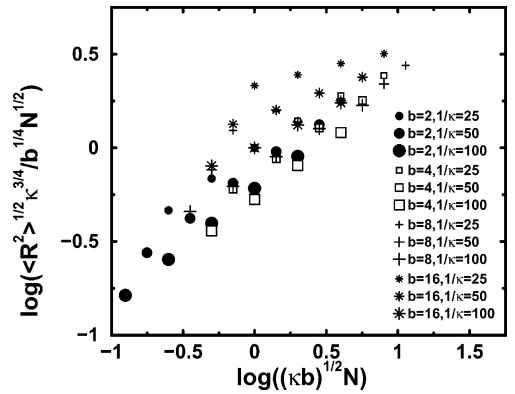


**Figure 3.** Figure 1 of ref 38 corrected, i.e., plotted as the intended representation of eq 43. Note that for each bond length $b$, one point $(x_0, y_0)$, corresponding to a particular $N$ and $\kappa$, has been chosen and the plot is really $\log(y/y_0)$ vs $\log(x/x_0)$, where $x$ and $y$ represent $(\langle R^2\rangle\kappa^2/(\kappa b)^{1/2}N)^{1/2}$ and $(\kappa b)^{1/2}N$, respectively (cf. eq 43). $b$ and $\kappa^{-1}$ are given in units of $l_B$. $\alpha = 1$ and $N = 16-256$.

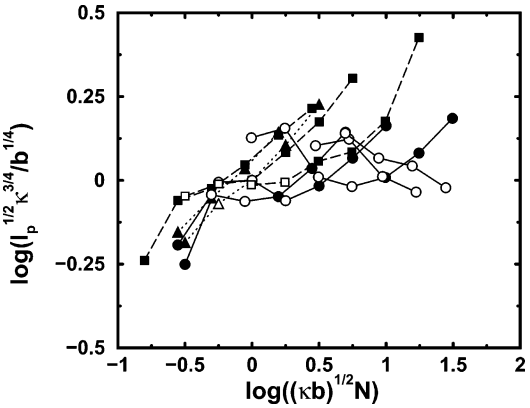


**Figure 4.** Same type of plot as in Figure 3, but using the projection length $l_{p,e}$ instead of $\langle R^2\rangle/N$ and the following data sets: $b = 3$ Å and $\alpha = 1$ with $N = 160-5000$ (circles and solid lines); $b = 12$ Å and $\alpha = 1$ with $N = 160-1000$ (squares and dashed lines); and $b = 12$ Å and $\alpha = 0.5$ with $N = 160-320$ (triangles and dotted lines). Open symbols denote points in the DH regime (see section 5.2). The lines join points with the same set of $N$, $b$, and $\alpha$, but different $\kappa^{-1}$, which ranges from 960 down to 1 Å.

to do.[38] In reality, however, $(\langle R^2\rangle\kappa^2N/(\kappa b)^{1/2})^{1/2}$ vs $(\kappa b)^{1/2}N$ was plotted instead. Furthermore, most of the data points where in the rodlike regime where $\langle R^2\rangle \sim N^2$ (independent of $\kappa$). Thus, with the bond length dependence factored out, LS, in effect, plotted $(\kappa^{1/2}N)^{3/2}$ vs $(\kappa^{1/2}N)$, which is indeed universal. This follows from simulations of my own, where I have repeated those of MK and have been able to reproduce the erroneous figure. In Figure 3, the data are plotted the way that was originally intended and they do not display any universal behavior.

A problem with the comparison is that the chains are rather short and the sought after DH regime is extremely narrow. $\langle R^2\rangle$ goes straight from the rodlike regime to the excluded volume regime. In principle, it should help to use the (extrapolated) projection length $l_p$, since it corresponds to $\langle R^2\rangle/N$ for infinitely long chains when the range of interactions is finite. Figure 4 shows the same type of plot with $l_p$ and longer chains. Now there are points that represent the DH regime and they are marked by open symbols, using the criteria presented in section 5.2 (cf. Figure 1b). This does not improve the situation, however. There is still no convergence to a universal function.

In short, the theory presented by Liverpool and Stapper does not apply to the three-dimensional case.

**7.2. Scaling Analysis.** In the analysis of Liverpool and Stapper, intermediate results were expressed as[39]

$$\langle R^2\rangle \sim b^2N^{2\nu_p}\mathcal{F}_1((\kappa b)^2N^{\nu_p/\nu_C}) \tag{46}$$

and

$$\langle R^2\rangle \sim \frac{b^2}{(\kappa b)^{4\nu_C}}\mathcal{F}_2((\kappa b)^{2\nu_C/\nu_p}N) \tag{47}$$

where $\nu_C = 1/2$.

These equations can be treated as general scaling laws with $\mathcal{F}_1(x)$ and $\mathcal{F}_2(x)$ representing power laws in certain limits. Knowing the $N$ dependence of $\langle R^2\rangle$ in these limits gives the $\kappa$ dependence. Since $\nu_p$ represents the exponent for the unscreened case, it is obvious from eq 46 that the behavior in this limit is just

$$\langle R^2\rangle \sim b^2N^{2\nu_p} \tag{48}$$

i.e., independent of $\kappa$ as expected.

In three-dimensions, the chain should be rodlike in the unscreened limit, i.e., $\nu_p = 1$. In the highly screened regime, the chain is expected to behave as a self-avoiding walk $\langle R^2\rangle \sim N^{6/5}$, using the Flory exponent $\nu = 3/5$, or as a Gaussian chain $\langle R^2\rangle \sim N$, if excluded volume interactions are neglected. Combining this with eq 46 or eq 47 gives

$$\langle R^2\rangle \sim \frac{b^{6/5}N^{6/5}}{\kappa^{4/5}} \tag{49}$$

with excluded volume interactions and

$$\langle R^2\rangle \sim \frac{bN}{\kappa} \tag{50}$$

without. This analysis was also performed by LS with the self-avoiding walk as the second limit.[39]

These scaling laws are the same as eqs 19−21 ($b$ is mainly included to adjust the dimensionality and should not be inferred as a bond length dependence), which have been shown not to give a good representation of a polyelectrolyte within the Debye−Hückel approximation (see also Section 5).[36,37]

Equation 49 was obtained by using Flory-type exponents. If we instead consistently use the renormalization group or des Cloizeaux-type exponents for the unscreened and excluded volume regimes, i.e., $\nu_p = 2$ and $\nu = 2/3$, respectively. We get

$$\langle R^2\rangle \sim \frac{b^{2/3}N^{4/3}}{\kappa^{4/3}} \tag{51}$$

which is the same behavior as in eq 41, obtained by Netz and Orland.[22]

In fact, eqs 46 and 47 represent a special case of an even more general scaling law, provided that consistent sets of exponents are used. To see this, let us go back to section 3.4.2 and note that the difference between the Flory-type result and the des Cloizeaux counterpart can be seen as the coefficients on the right-hand side of the balance of powers

$$2 - \nu\lambda = a\nu + c \tag{52}$$

where the Flory approach gives $a = 2$ and $c = -1$, while $a = c = 0$ yields the renormalization group or des Cloizeaux exponents. To balance the coefficients of $N$, we note that $\nu$ follows from the transformation $R \sim BN^{\nu}$. The coefficient with

$R^{-\lambda}$ implied on the left-hand side is made dimensionless by the coupling parameter $\Lambda$, while $R^a$ of the right-hand side requires $b^{-a}$. Thus, we get the general expression

$$R \sim \Lambda^{1/(\lambda+a)} b^{a/(\lambda+a)} N^{(2-c)/(\lambda+a)} \tag{53}$$

Now let us assume that we only have two regimes, one where $\lambda = d - 2$ (Coulomb interactions in an unscreened regime) and another with arbitrary $\lambda$. This behavior can be combined into the scaling law

$$R \sim R_C \mathcal{F}\left(\frac{R_\lambda}{R_C}\right) \tag{54}$$

where $\mathcal{F}(x) = 1$ in the Coulomb regime, where $R \sim R_C$, and $\mathcal{F}(x) = x$ in the regime with arbitrary $\lambda$. After inserting eq 53 for the two cases, the result is

$$R \sim \Lambda_C^{1/(d-2+a)} b^{a/(1+a)} N^{(2-c)/(d-2+a)} \mathcal{F}\left(\left[\frac{[\Lambda_\lambda^{d-2+a} b^{a(d-2-\lambda)} N^{(2-c)(d-2-\lambda)}]}{\Lambda_C^{(\lambda+a)}}\right]^{1/[(\lambda+a)(d-2+a)]}\right) \tag{55}$$

Using $\nu_p = (2 - c)/(d - 2 + a)$ and switching to a new function $\mathcal{G}(x) = \mathcal{F}(x^{1/(\lambda+a)})$, this can be rewritten as

$$R \sim \Lambda_C^{\nu_p/(2-c)} b^{a\nu_p/(2-c)} N^{\nu_p} \mathcal{G}\left(\frac{\Lambda_\lambda b^{a\nu_p(d-2-\lambda)/(2-c)} N^{\nu_p(d-2-\lambda)}}{\Lambda_C^{\nu_p(\lambda+a)/(2-c)}}\right) \tag{56}$$

Let us take $\lambda = d$ and $\Lambda_\lambda \sim \kappa^{-2}$, which is the result of an integral over the screened Coulomb potential also when it is generalized to dimension $d$ (LS[39] list the generalized potentials for $d = 2-6$). If we retain only $N$ and $\kappa$ as true parameters and compensate the units with the nominal length $b$, we get

$$R \sim b N^{\nu_p} \mathcal{G}\left(\frac{1}{(\kappa b)^2 N^{2\nu_p}}\right) \tag{57}$$

which is obviously equivalent to eq 46 if $\mathcal{F}_1(x) = [\mathcal{G}(1/x)]^2$.

In other words, treated as a scaling analysis, the theory of Liverpool and Stapper boils down to an approach were the screened Coulomb interactions are treated as spherical excluded volume interactions, just like in the theories of Bratko and Dawson[51] and Netz and Orland.[22] With the most realistic exponents in $d = 3$, i.e., $\nu_p = 1$ for the unscreened case and $\nu = 3/5$ for the highly screened regime, the intermediate scaling results are on par with a simple Flory approach.

## 8. Conclusions

Simulations of very long, flexible polyelectrolytes with screened Coulomb interactions display three regimes with respect to the screening length $\kappa^{-1}$. In the unscreened regime, i.e., when screening length is large compared to the chain size, the chain has a rodlike character. When $\kappa^{-1}$ is comparable to the chain size, the chain is semiflexible with a projection length approaching the OSFKK prediction $l_p \sim \kappa^{-2}$. In fact, the expression presented by Odijk, eq 3, contains a qualitatively correct description of both regimes, as long as the chain is rather stiff. When the screening length is short, corresponding to high concentrations of added salt, the chain is flexible enough to loop back on itself, which means that occasional contacts between distant parts of the chain give rise to increased long-range correlations, so-called excluded volume effects. In this regime $l_p \sim \kappa^{-1.2}$.

The intermediate, semiflexible regime is only fully developed for very long chains with strong electrostatic interactions. For shorter chains, the unscreened regime crosses quickly over to the excluded volume regime, which is why simulations have generally reported a projection length depending close to linearly on the screening length, until very recently.[36,37] It is likely that the experimental observation of $l_p \sim \kappa^{-1}$ for flexible chains represents the behavior of an excluded volume regime in a similar way.

As for the internal behavior, it is important to recognize that it is different on different length scales. The chain retains a high degree of flexibility on short length scales, while the electrostatic interactions add stiffness at longer range. Phrased differently, the orientational correlation function has a fast short-range decay and a slower long-range decay. This behavior is not consistent with a wormlike chain, but can be described by a modification to a two-parameter model, like the snakelike chain, eq 9, although with excluded volume effects, the long-range decay is no longer exponential.

A simple scaling argument based on OSF theory and the ideas of Odijk and Houwaart is in perfect agreement with the simulation result $l_p \sim \kappa^{-1.2}$ in the excluded volume regime. However, one of the basic assumptions, namely that the chain is characterized by $l_p \sim \kappa^{-2}$ in the absence of the excluded volume effects, is not entirely correct. Simulation results selected to avoid these effects give $l_p \sim \kappa^{-1.6}$. A different approach is therefore needed to describe the details of the behavior.

One-parameter variational methods cannot simultaneously account for the short-range flexibility and the long-range stiffness that is intrinsic to flexible polyelectrolytes. With the usual Gaussian element in the approach, there is an emphasis on flexibility and the result is $l_p \sim \kappa^{-1}$ without excluded volume effects, in contrast to the perturbative method of OSF theory, which focuses on rigidity and gives $l_p \sim \kappa^{-2}$. When the length scales are separated in the form of the traditional blob picture, the results depend on the approximation used for the chain of blobs, which represents a rescaled form of a one-parameter model. Results on the level of a one-parameter model are also obtained from a more general approach, if the behavior is assumed to be the same on all length scales.

It has been argued,[38,39] on the basis of a field-theoretic renormalization group theory, that there should be no simple power law when the screening length is comparable to the chain size. An analysis of the consequences of the theory shows that the results are not valid in the three-dimensional case. The support from simulations that the theory appeared to enjoy[38] was due to an unfortunate mistake in the preparation of a figure. A corrected plot does not show any universal behavior, in contrast to the prediction of the theory. On a scaling level, the theory corresponds to treating the screened Coulomb interactions as excluded volume interactions and, with a realistic set of exponents, reproduces the results of a simple Flory approach.

**Acknowledgment.** I would like to thank Ralf Everaers, Boris Shklovskii, Tanniemola Liverpool, Kurt Kremer, Uwe Micka, and Roland Winkler for stimulating discussions and correspondence.

## References and Notes

(1) Debye, P.; Hückel, E. *Phys. Z.* **1923**, *24*, 185−206.
(2) Hermans, J. J.; Overbeek, J. T. G. *Recl. Trav. Chim. Pays-Bas* **1948**, *67*, 761−776.
(3) Katchalsky, A. *J. Polym. Sci.* **1951**, *7*, 393−412.

(4) Katchalsky, A.; Lifson, S. *J. Polym. Sci.* **1953**, *11*, 409−423.
(5) Muthukumar, M. *J. Chem. Phys.* **1987**, *86*, 7230−7235.
(6) Muthukumar, M. *J. Chem. Phys.* **1996**, *105*, 5183−5199.
(7) Odijk, T. *J. Polym. Sci., Polym. Phys. Ed.* **1977**, *15*, 477−483.
(8) Skolnick, J.; Fixman, M. *Macromolecules* **1977**, *10*, 944−948.
(9) Kratky, O.; Porod, G. *Recl. Trav. Chim. Pays-Bas* **1949**, *68*, 1106−1122.
(10) Ullner, M. In *Handbook of Polyelectrolytes and Their Applications*; Tripathy, S. J. K., Nalwa, H. S., Eds.; American Scientific Publishers: Los Angeles, 2002; Vol. 3, p 271−308.
(11) Saitô, N.; Takahashi, K.; Yunoki, Y. *J. Phys. Soc. Jpn.* **1967**, *22*, 219−226.
(12) Ullner, M.; Woodward, C. E. *Macromolecules* **2002**, *35*, 1437−1445.
(13) Micka, U.; Kremer, K. *Europhys. Lett.* **1997**, *38*, 279−284.
(14) Ullner, M.; Jönsson, B.; Peterson, C.; Sommelius, O.; Söderberg, B. *J. Chem. Phys.* **1997**, *107*, 1279−1287.
(15) de Gennes, P. G.; Pincus, P.; Velasco, R. M.; Brochard, F. *J. Phys.* **1976**, *37*, 1461−1473.
(16) Khokhlov, A. R.; Khachaturian, K. A. *Polymer* **1982**, *23*, 1742−1750.
(17) Barrat, J.-L.; Joanny, J.-F. *Europhys. Lett.* **1993**, *24*, 333−338.
(18) de Gennes, P.-G. *Scaling Concepts in Polymer Physics*; Cornell University Press: Ithaca, NY, 1979.
(19) Barrat, J.-L.; Joanny, J.-F. *Adv. Chem. Phys.* **1996**, *94*, 1−66.
(20) Li, H.; Witten, T. A. *Macromolecules* **1995**, *28*, 5921−5927.
(21) Ha, B.-Y.; Thirumalai, D. *J. Chem. Phys.* **1999**, *110*, 7533−7541.
(22) Netz, R. R.; Orland, H. *Eur. Phys. J. B* **1999**, *8*, 81−98.
(23) Podgornik, R.; Hansen, P. L.; Parsegian, V. A. *J. Chem. Phys.* **2000**, *113*, 9343−9350.
(24) Hansen, P. L.; Podgornik, R. *J. Chem. Phys.* **2001**, *114*, 8637−8648.
(25) Schmidt, M. *Macromolecules* **1991**, *24*, 5361−5364.
(26) Ha, B.-Y.; Thirumalai, D. *Macromolecules* **1995**, *28*, 577−581.
(27) Reed, C. E.; Reed, W. F. *J. Chem. Phys.* **1991**, *94*, 8479−8486.
(28) Barrat, J.-L.; Boyer, D. *J. Phys. II* **1993**, *3*, 343−356.
(29) Seidel, C. *Ber. Bunsen-Ges. Phys. Chem.* **1996**, *100*, 757−763.
(30) Tricot, M. *Macromolecules* **1984**, *17*, 1698−1704.
(31) Ghosh, S.; Li, X.; Reed, C. E.; Reed, W. F. *Biopolymers* **1990**, *30*, 1101−1112.
(32) Reed, W. F.; Ghosh, S.; Medjahdi, G.; Francois, J. *Macromolecules* **1991**, *24*, 6189−6198.
(33) Degiorgio, V.; Mantegazza, F.; Piazza, R. *Europhys. Lett.* **1991**, *15*, 75−80.
(34) Sorci, G. A.; Reed, W. F. *Macromolecules* **2002**, *35*, 5218−5227.
(35) Micka, U.; Kremer, K. *Phys. Rev. E* **1996**, *54*, 2653−2662.
(36) Everaers, R.; Milchev, A.; Yamakov, V. *Eur. Phys. J. E* **2002**, *8*, 3−14.
(37) Nguyen, T. T.; Shklovskii, B. I. *Phys. Rev. E* **2002**, *66*, 021801.
(38) Liverpool, T. B.; Stapper, M. *Europhys. Lett.* **1997**, *40*, 485−490.
(39) Liverpool, T. B.; Stapper, M. *Eur. Phys. J. E* **2001**, *5*, 359−375.
(40) Fisher, M. E. *J. Phys. Soc. Jpn., Suppl.* **1969**, *26*, 44−45.
(41) Flory, P. J. *J. Chem. Phys.* **1949**, *17*, 303−310.
(42) Flory, P. J.; Fox, T. G., Jr. *J. Am. Chem. Soc.* **1951**, *73*, 1904−1908.
(43) Kuhn, W.; Künzle, O.; Katchalsky, A. *Helv. Chim. Acta* **1948**, *31*, 1994−2037.
(44) Katchalsky, A.; Künzle, O.; Kuhn, W. *J. Polym. Sci.* **1950**, *5*, 283−300.
(45) Odijk, T.; Houwaart, A. C. *J. Polym. Sci., Polym. Phys. Ed.* **1978**, *16*, 627−639.
(46) Yamakawa, H. *Modern Theory of Polymer Solutions*; Harper and Row: New York, 1971.
(47) Ullner, M.; Jönsson, B. *Macromolecules* **1996**, *29*, 6645−6655.
(48) Pfeuty, P.; Velasco, R. M.; de Gennes, P. G. *J. Phys. (Paris)* **1977**, *38*, L5−L7.
(49) des Cloizeaux, J. *J. Phys. Soc. Jpn., Suppl.* **1969**, *26*, 42−45.
(50) des Cloizeaux, J. *J. Phys.* **1970**, *31*, 715−736.
(51) Bratko, D.; Dawson, K. A. *J. Chem. Phys.* **1993**, *99*, 5352−5361.
(52) Jug, G.; Rickayzen, G. *J. Phys. A* **1981**, *14*, 1357−1381.
(53) Bouchaud, J.-P.; Mézard, M.; Parisi, G.; Yedidia, J. S. *J. Phys. A: Math. Gen.* **1991**, *24*, L1025−L1030.
(54) Marinari, E.; Parisi, G. *Europhys. Lett.* **1991**, *15*, 721−724.
(55) Kurata, M.; Stockmayer, W. H.; Roig, A. *J. Chem. Phys.* **1960**, *33*, 151−155.
(56) Reiss, H. *J. Chem. Phys.* **1967**, *47*, 186−194.
(57) Metropolis, N. A.; Rosenbluth, A. W.; Rosenbluth, M. N.; Teller, A.; Teller, E. *J. Chem. Phys.* **1953**, *21*, 1087−1097.
(58) Lal, M. *Mol. Phys.* **1969**, *17*, 57−64.
(59) Madras, N.; Sokal, A. D. *J. Stat. Phys.* **1988**, *50*, 109−186.
(60) Ullner, M.; Jönsson, B.; Söderberg, B.; Peterson, C. *J. Chem. Phys.* **1996**, *104*, 3048−3057.
(61) Erratum: In ref 12, the pivot rotation around a random direction was incorrectly described as being around a bond.
(62) Reed, C. E.; Reed, W. F. *J. Chem. Phys.* **1990**, *92*, 6916−6926.
(63) Reed, C. E.; Reed, W. F. *J. Chem. Phys.* **1992**, *97*, 7766−7776.
(64) Grosberg, A. Y.; Khokhlov, A. R. *Statistical Physics of Macromolecules*; AIP Press: New York, 1994.
(65) Edwards, S. F.; Singh, P. *J. Chem. Soc., Faraday Trans. 2* **1979**, *75*, 1001−1019.
(66) Jönsson, B.; Peterson, C.; Söderberg, B. *J. Phys. Chem.* **1995**, *99*, 1251−1266.
(67) Lagowski, J. B.; Noolandi, J.; Nickel, B. *J. Chem. Phys.* **1991**, *95*, 1266−1269.
(68) Ghosh, K.; Carri, G. A.; Muthukumar, M. *J. Chem. Phys.* **2001**, *115*, 4367−4375.
(69) Migliorini, G.; Rostiashvili, V. G.; Vilgis, T. A. *Eur. Phys. J. E* **2001**, *4*, 475−487.
(70) Jönsson, B.; Peterson, C.; Söderberg, B. *Phys. Rev. Lett.* **1993**, *71*, 376−379.
(71) Jönsson, B.; Ullner, M.; Peterson, C.; Sommelius, O.; Söderberg, B. *J. Phys. Chem.* **1996**, *100*, 409−417.
(72) Jug, G. *J. Phys. (Paris)* **1981**, *42*, L409−L412.
(73) Jug, G. *Ann. Phys. (N.Y.)* **1982**, *142*, 140−184.
(74) Baumgärtner, A. *J. Physique Lett.* **1984**, *45*, L515−L521.
(75) Liverpool, T. B. Personal communication.